P4.10 SOUND PROPAGATION OBSERVATIONS DURING THE CASES-99 EXPERIMENT

D. Keith Wilson,* John M. Noble, and Mark A. Coleman
U. S. Army Research Laboratory, Adelphi, Maryland

1. INTRODUCTION

Some basic features of sound propagation at night are well known. Most importantly, nocturnal inversions tend to trap sound energy in a ground-based duct, allowing sound to propagate efficiently over long distances (Delany, 1977; Embleton, 1996). Beyond this simple fact, however, there is still much to be understood. For example, how do sound levels typically evolve over the course of a night during fair weather? How high in the atmosphere do horizontally transmitted signals travel before returning to the ground? How stable are the propagating modes in the ground-based duct? Which atmospheric phenomena play a primary role in driving acoustic signal variability? Can the effects of intermittent turbulent activity and gravity waves be observed in acoustic signals?

In this paper, we describe a sound propagation experiment that was undertaken in conjunction with CASES-99 (Poulos et al., 2001) in the hope of addressing some of these questions. The comprehensive boundary-layer measurements made during CASES-99 provide a unique opportunity to relate the acoustic signal behavior to the underlying atmosphere. Our experimental set-up for sound propagation is described in Section 2. Results over the course of Intensive Observation Periods (IOP's) 6 and 7 are provided in Section 3, with an in-depth examination of two of the strong events occuring during IOP 7.

2. EXPERIMENT

The sound transmission path was nominally horizontal over gently sloped terrain. The single sound source was positioned roughly 1.8 km southwest of the main 60-m tower, with the transmission path running due north. A series of five 6-m towers placed at distances between 361 and 1180 m from the source, as shown in Figure 1. Each tower had microphones at heights of 0.5, 1, 2, and 3 m. There were also 3 transverse linear arrays placed on the ground at various distances out to 1300 m from the speaker.

Propagation trials were conducted during IOP's 3 through 7. The sound source for IOP 3 consisted of a propane cannon, which generates a repeatable, impulsive signal. During the remaining IOP's, a continuous, 50-Hz square wave was broadcast from a loudspeaker at 1-m height. The square wave includes higher odd harmonics of the 50-Hz fundamental (150 Hz, 250 Hz, ...).

The microphone signals were sampled at 12 kHz and recorded onto digital audio tape. Due to the huge amount of data being stored, the tapes had to be changed roughly every 2 hours. A pair of 2-hour sessions were conducted for IOP's 3, 4, and 5. For IOP's 6 and 7, the tapes were exchanged regularly througout the night, providing a nearly continous record of the sound level from dusk until sunrise. In this paper, we focus on these latter two IOP's.

Signal levels were determined by FFT processing of 5-s (60,000-sample) segments with an 80% overlap. The sound energy (or, more precisely, the squared sound pressure, which is proportional to the sound energy) at each frequency of interest f was then determined by adding the squared magnitudes of all bins within ± 2.5 Hz of f. This interval was large enough to capture all spreading of the sound energy in frequency due to Doppler shifts from random scattering, which was found to be well less than 1 Hz. As is traditional in acoustics, the energy was converted to decibels by taking the base-ten logarithm and multiplying by 10. This quantity is referred to as the sound level.

3. RESULTS

3.1 Effective Sound Speed

For nearly horizontal propagation paths such as in the present experiment, the behavior of the acoustic signal is determined primarily by the "effective" sound speed field $c_{\rm eff}$, which is the sum of the actual sound speed c and the component of the wind velocity in the nominal propagation direction (Ostashev, 1997). Since our propagation path is due north, $c_{\rm eff} = c + v$, where v is the northward wind component. The sound speed is calculated from the equation $c = \sqrt{\gamma_d R_d T\,(1 + 0.511r)}$, where γ_d is the specific heat ratio for dry air, R_d is the gas constant for dry air, T is temperature, and r is the water vapor mixing ratio (Ostashev, 1997).

Figures 2 and 3 show the effective sound speed during IOP's 6 and 7 at several heights on the main 60-m tower (Poulos et al., 2001). (The heights shown

* *Corresponding author address*: D. Keith Wilson, U.S. Army Research Laboratory, ATTN: AMSRL-CI-EE, 2800 Powder Mill Rd., Adelphi, MD 20783-1197; e-mail: dkwilson@arl.army.mil.

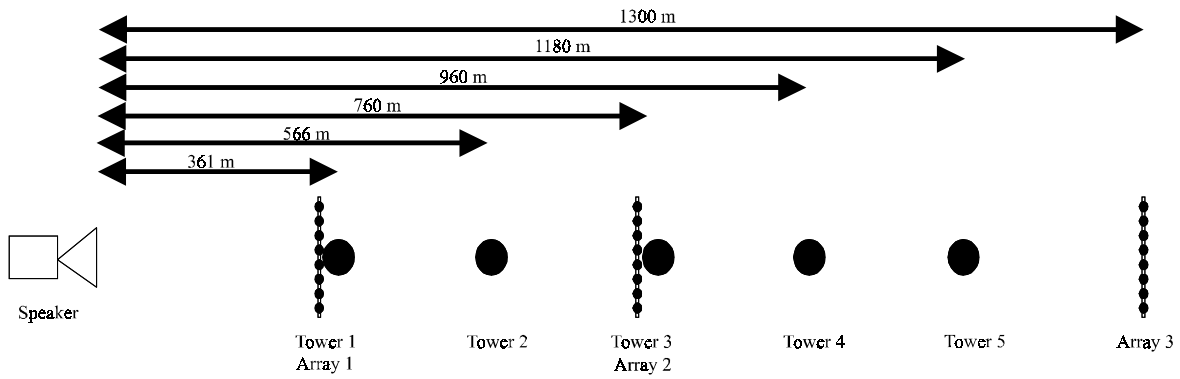

Figure 1: Layout of the sound-propagation path.

are from 5 to 55 m, in 10-m intervals. Standard slow-response sensors were used in all cases, except for the winds at 5 and 55 m, where sonic anemometer data were used.) A positive gradient in c_{eff} causes downward refraction and ducting of sound near the ground, whereas a negative gradient causes upward refraction and acoustic "shadow" formation. Roughly similar patterns to the evolution of the c_{eff} profile are evident during both IOP's. The evening starts with a weak, negative gradient in c_{eff}. This is primarily due to upwind propagation: examination of the wind data show that propagation was upwind until about 0630 UTC (0130 LST) on both nights, at which time it shifted to downwind. Between roughly 0200 and 0500 UTC, a transition occurs to very strong, positive gradients in c_{eff}. This transition is due to primarily to shifting wind direction combined with the temperature inversion.

For IOP 7, a very strong event occurs between 0130 and 0200 UTC. Sun et al. (2000) describe this as a density current. A second event of very short duration occurs around 0645 UTC. Immediately before the record ends at 1230 UTC, a third strong event occurs. Although there is much variation in the c_{eff} profile during IOP 6, there appear to be no counterparts to the three events in IOP 7.

3.2 Nocturnal Behavior of Sound Levels

Complete processed sound levels for 50, 150, 250, and 350 Hz at the 0.5-m microphone on tower 2 (566 m) are shown in Figs. 4 and 5. These figures combine all the recordings for IOP 6 and IOP 7, respectively. The curves have been arbitrarily offset along the vertical axis for better visibility.

During IOP 6, there is a very loose tendency for the sound levels to increase from about 0000 UTC to 0230 UTC, decrease from 0230 to 0500 UTC, and then increase once again until sunrise. The reason for decreasing sound levels after 0230 UTC is not evident from the c_{eff} profile (Fig. 2). The likely cause is a shifting interference pattern between the propagating acoustic modes trapped near the ground; we plan to examine this hypothesis in more detail. Superimposed on this general behavior are many strong fading episodes where the sound levels decrease as much as 15 dB over periods ranging from a few minutes to an hour. These variations in sound level are most pronounced at higher frequency.

The signal behavior during IOP 7 is similar to IOP 6, although there is a trend for gradually increasing sound levels at all frequencies throughout the night.

3.3 Discrete Events during IOP 7

In this subsection, we consider the behavior of the acoustical signal during the strong events of IOP 7. The two-hour recording including event 1 is shown in Fig. 6; event 3 is shown in Fig. 7. The 50-Hz signal at the 2-m microphones on towers 2, 3, and 5 (570, 760, and 1170 m, respectively) is shown. We found that event 2, which was the weakest of the three, had no obvious impact on the acoustic signals.

In Fig. 6, the sound levels peak at 0140 UTC and then start to oscillate with a period of about 15 min. This behavior is remarkably consistent among all microphones and clearly coincides with observations of event 1.

Event 3 and the period leading up to it (Fig. 7) produce more complex behavior in the sound levels. We observe a deep fading in the sound level at 1130 UTC at the more distant microphones. At the same time, the sound level at the near microphone attains a local maximimum. Comparing with Fig. 3, we see that this behavior corresponds to an increase in the effective sound speed above 15 m. Shortly after 1215 UTC, near the onset of event 3, very rapid fluctuations in the sound level are observed at all microphones. These fluctuations are particularly strong at the two more distant microphones.

We have attempted to predict the time histories of the pressure signals during events 1 and 3 with a numerical sound propagation code (Wilson, 1993). The

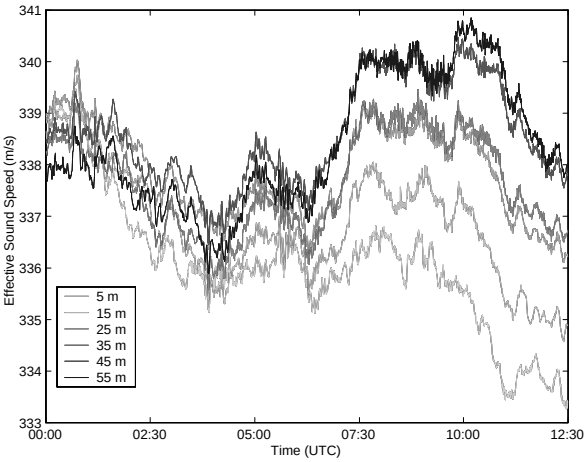

Figure 2: Effective sound speed at several heights on the main tower during IOP 6.

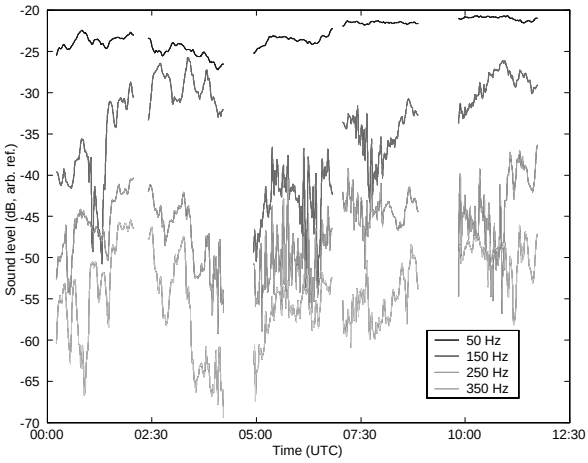

Figure 4: Sound levels at the 0.5-m microphone on tower 2 during IOP 6.

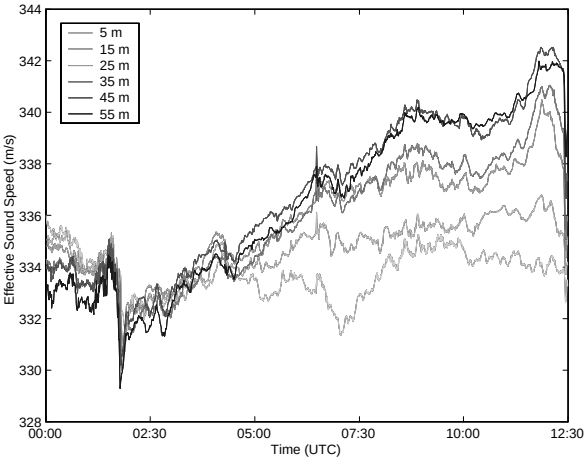

Figure 3: Effective sound speed at several heights on the main tower during IOP 7.

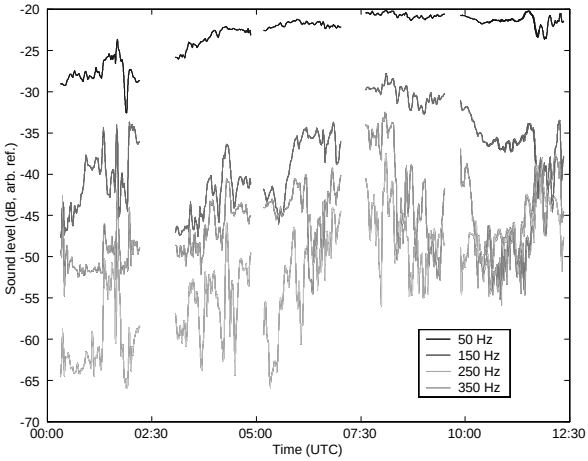

Figure 5: Sound levels at the 0.5-m microphone on tower 2 during IOP 7.

temperatures recorded at the main tower were used as input, under the assumption that the temperature follows the adiabatic lapse rate above the highest sensors on the main tower. Although there is some qualitative agreement between the observed sound levels and predictions, the observed variations are much stronger than in the predictions. For example, during Event 1, the signal level at tower 5 is observed to drop by about 16 dB from a maximum at 0140 to a minimum at 0152. The numerical calculations predict a drop of about 6 dB during this time. This discrepency is very likely due to atmospheric structure above the tower.

4. CONCLUSION

The sound observations during CASES-99 have provided unique insights into the mechanisms of propagation at night. The evolution of the received acoustic signal energy appears to be determined by a combination of strengthening of the nocturnal inversion, strong discrete events (density currents and solitary waves), and signal variations likely attributable to shifting interference patterns in the propagating acoustic modes. Detailed numerical modeling of the sound propagation during CASES-99 is inhibited by the need for rapidly updated wind and temperature profile data above the main 60-m tower. We are currently considering methods for merging the available raobs with the tower data.

The very dramatic sensitivity of sound waves to changes in nocturnal boundary layer structure suggests possibilities for remote sensing modalities that are distinct from sodar (Chunchuzov et al., 1997; Wilson et al., 2001), provided that the important propagation mechanisms can be identified more clearly. Such schemes have

the potential for continuously monitoring the wind and temperature profiles at heights well above most instrumented towers.

ACKNOWLEDGMENTS

We thank S. Burns for his help in accessing the CASES-99 tower data and J. Sun for discussing preliminary results on the three events during IOP 7. We are also grateful to many other CASES-99 participants for the insights they have shared on various occassions, including the workshops sponsored by W. Bach (Army Research Office).

References

Chunchuzov, I. P., A. I. Otrezov, I. V. Petenko, V. N. Tovchigrechko, A. I. Svertilov, A. L. Fogel, and V. E. Fridman, 1997: Travel time fluctuations of acoustic pulses propagating in the atmospheric boundary layer. *Izv. Atmos. Ocean. Phys.*, **3**, 324–338.

Delany, M. E., 1977: Sound propagation in the atmosphere: a historical review. *Acustica*, **38**, 201–223.

Embleton, T. F. W., 1996: Tutorial on sound propagation outdoors. *J. Acoust. Soc. Am.*, **100**, 31–48.

Ostashev, V. E., 1997: *Acoustics in Moving Inhomogeneous Media*. E & FN Spon, London.

Poulos, G. S., W. Blumen, D. C. Fritts, J. K. Lundquist, J. Sun, S. P. Burns, C. Nappo, R. Banta, R. Newsom, J. Cuxart, E. Terradellas, B. Balsley, and M. Jensen, 2001: CASES-99: A comprehensive investigation of the stable nocturnal boundary layer. *Bull. Amer. Meteor. Soc.* (submitted).

Sun, J., S. Burns, D. Lenschow, and Q. Oosterhuis, 2000: Turbulence intermittency in the stable boundary layer. In *14th Symposium on Boundary Layer and Turbulence*, American Meteorological Society, Boston, 329–331.

Wilson, D. K., 1993: Sound field computations in a stratified, moving medium. *J. Acoust. Soc. Am.*, **94**, 400–407.

Wilson, D. K., A. Ziemann, V. E. Ostashev, and A. G. Voronovich, 2001: An overview of acoustic travel-time tomography in the atmosphere and its potential applications. *Acustica*, **87**, 721–730.

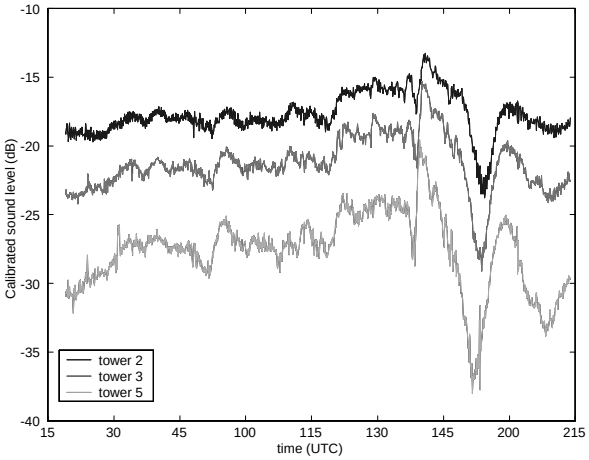

Figure 6: Sound levels at the 2-m microphones on towers 2, 3, and 5, over a two-hour period including Event 1.

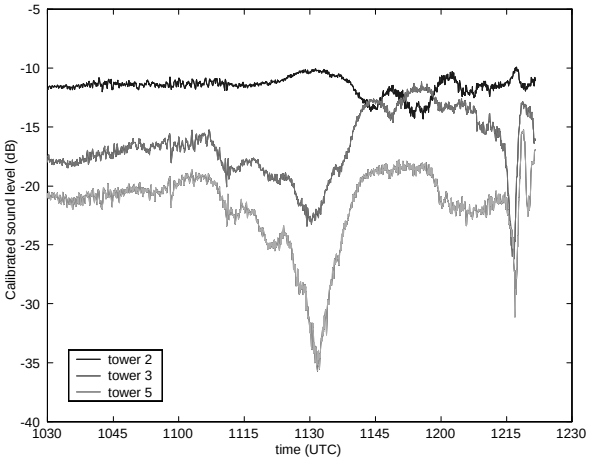

Figure 7: Sound levels at the 2-m microphones on towers 2, 3, and 5, over a two-hour period including Event 3.